Available online at www.sciencedirect.com
SCIENCE DIRECT®
Journal of Nuclear Materials 347 (2005) 207–216
journal of nuclear materials
www.elsevier.com/locate/jnucmat

Development of refractory armored silicon carbide by infrared transient liquid phase processing

Tatsuya Hinoki *, Lance L. Snead, Craig A. Blue

Metals and Ceramics Division, Oak Ridge National Laboratory, 1 Bethel Valley Road, Oak Ridge, TN 37830, USA

Abstract

Tungsten (W) and molybdenum (Mo) were coated on silicon carbide (SiC) for use as a refractory armor using a high power plasma arc lamp at powers up to 23.5 MW/m^2 in an argon flow environment. Both tungsten powder and molybdenum powder melted and formed coating layers on silicon carbide within a few seconds. The effect of substrate pre-treatment (vapor deposition of titanium (Ti) and tungsten, and annealing) and sample heating conditions on microstructure of the coating and coating/substrate interface were investigated. The microstructure was observed by scanning electron microscopy (SEM) and optical microscopy (OM). The mechanical properties of the coated materials were evaluated by four-point flexural tests. A strong tungsten coating was successfully applied to the silicon carbide substrate. Tungsten vapor deposition and pre-heating at 5.2 MW/m^2 made for a refractory layer containing no cracks propagating into the silicon carbide substrate. The tungsten coating was formed without the thick reaction layer. For this study, small tungsten carbide grains were observed adjacent to the interface in all conditions. In addition, relatively large, widely scattered tungsten carbide grains and a eutectic structure of tungsten and silicon were observed through the thickness in the coatings formed at lower powers and longer heating times. The strength of the silicon carbide substrate was somewhat decreased as a result of the processing. Vapor deposition of tungsten prior to powder coating helped prevent this degradation. In contrast, molybdenum coating was more challenging than tungsten coating due to the larger coefficient of thermal expansion (CTE) mismatch as compared to tungsten and silicon carbide. From this work it is concluded that refractory armoring of silicon carbide by Infrared Transient Liquid Phase Processing is possible. The tungsten armored silicon carbide samples proved uniform, strong, and capable of withstanding thermal fatigue testing.

1. Introduction

Silicon carbide can be used in extremely harsh environments due to its excellent thermal, mechanical, and chemical stability. Silicon carbide also provides exceptionally low radioactivity following neutron irradiation [1]. The intrinsic features of silicon carbide make silicon carbide fiber-reinforced silicon carbide matrix composites (SiC/SiC composites) a very attractive structural material for nuclear application [2].

Refractory armored materials have been previously considered in the magnetic fusion energy

* Corresponding author. Present address: Institute of Advanced Energy, Kyoto University, Gokasho, Uji, Kyoto 611-0011, Japan. Tel.: +81 774 38 3461; fax: +81 774 38 3467.
E-mail address: hinoki@iae.kyoto-u.ac.jp (T. Hinoki).

0022-3115/$ - see front matter © 2005 Elsevier B.V. All rights reserved.
doi:10.1016/j.jnucmat.2005.08.020

community to reduce the introduction of power-sapping impurities into the plasma [3,4] and to reduce erosion. Recently, refractory armored materials have been considered for inertial fusion energy systems as a means to absorb and handle the very high impulse heat loading expected. To select the refractory armor material for silicon carbide, CTE is one key to obtaining a strong bond between substrate and refractory armor, since CTE mismatch causes residual thermal stress at the interface at high temperature. Considering the CTE mismatch and melting point, tungsten and molybdenum were selected as potential refractory armor materials for silicon carbide. Table 1 shows the thermal properties of silicon carbide [5], tungsten and molybdenum [6].

Although there are many techniques to apply refractory metals to ceramic substrates including physical vapor deposition, chemical vapor deposition and thermal spraying, the bonding strength between the substrate and layers produced with those techniques is low. Moreover, most of the techniques require long processing times above the reaction temperature of substrate material and coating material inducing thick reaction layers [7–9], which causes residual thermal stress and crack initiation due to CTE mismatch. A novel approach to forming this refractory layer using the Oak Ridge National Laboratory (ORNL) 300 kW infrared plasma arc lamp (IR processing) [10] is applied to mitigate these problems. This facility can apply up to 35 MW/m^2. Power can be delivered in a scan mode (scanning beam over sample) as wide as 0.35 m. The assumption driving application of this system for SiC/W was that by applying transient infrared power a layer of tungsten powder could melt and react with the surface of the silicon carbide while keeping the bulk silicon carbide below its sublimation temperature. The objective of this work is to develop refractory armor on silicon carbide by IR processing for fusion applications.

2. Experimental

The substrate material for this study was Hexoloy® SA [5] silicon carbide (sintered α-SiC). Substrates with dimension 25 mm (long) × 15 mm (wide) × 3 mm (thick) for standard specimens and 50 mm (long) × 4 mm (wide) × 3 mm (thick) for flexural bars were machined from plate. The refractory armor materials, tungsten powder or molybdenum powder of 3 μm average particle size, were sprayed on the silicon carbide to an approximate thickness of 200 μm. Several kinds of substrate pre-treatments including physical vapor deposition of titanium, tungsten for tungsten coating and molybdenum for molybdenum coating, and pre-melt substrate annealing were applied to form thin tungsten or molybdenum layers prior to infrared melting of the powder. The thin tungsten or molybdenum layer was intended to enhance bonding with armor coating formed by melting powder. The titanium was used to increase wettability. The annealing was applied to enhance bonding between the thin layer and substrate. The thicknesses of vapor deposition of titanium, tungsten and molybdenum were 0.20, 2.00 and 1.18 μm, respectively. The annealing temperatures after the vapor deposition were 1300 °C or 1500 °C for 72 h in a vacuum. The conditions of the pre-treatments are summarized in Table 2.

The plasma arc lamp used by IR processing is mounted on a Cincinnati-Milacron model T3-776 robotic arm. Using the robotic arm in conjunction with the Plasma Arc Lamp allows for a variety of experiments to be performed in a short amount of time. The powder on silicon carbide was heated by the lamp with 23.5 MW/m^2 for 2–5 s in an argon flow environment at atmospheric pressure. Pre-heating and post-heating at lower power (5.2–13.1 MW/m^2) for 6–20 s were also applied to optimize the IR processing conditions at various conditions. The powder on silicon carbide was also heated by scanning of the lamp with 17.0–23.5 MW/m^2 in an

Table 1
Thermal Properties of substrate and coating materials used in this work

Material	CTE (RT, 10^{-6}/K)	Melting point (°C)	Thermal conductivity (RT, W/mK)
Hexoloy SA SiC	4.02	2797 (α-SiC)	125.6
W	4.4	3370	163.3
Mo	5.35	2617	138

Table 2
Pre-treatment conditions

Vapor deposition (μm)	Annealing (°C)
W (2.00) or Mo (1.18)	
Ti (0.20) + W (2.00) or Mo (1.18)	
W (2.00) or Mo (1.18)	1300 (72 h)
Ti (0.20) + W (2.00) or Mo (1.18)	1300 (72 h)
W (2.00) or Mo (1.18)	1500 (72 h)
Ti (0.20) + W (2.00) or Mo (1.18)	1500 (72 h)

argon flow environment with atmospheric pressure. The scanning speed used was 5.0–12.0 mm/s. The effective heating area for the lamp used was approximately 30 × 10 mm. So the effective heating area by the scanning mode was 30 mm × scanning length.

The tungsten coated silicon carbide was sliced, and the coating and interface were observed by FE-SEM with energy dispersive X-ray spectroscopy (EDS) and OM. Mechanical properties of the tungsten coated silicon carbide were evaluated by four-point flexural tests with the coated side at tension, according to ASTM C1341. The support span and the loading span were 40 and 20 mm, respectively. The crosshead speed was 10 μm/s.

3. Result and discussion

3.1. Tungsten coating

Tungsten powder on silicon carbide melted in a couple of seconds by IR processing and formed a coating on silicon carbide. An OM image is given in Fig. 1, along with a micrograph of the as-machined substrate, to allow comparison of the surface roughness. In all specimens, including specimens with vapor deposited tungsten, a rough interface was observed. It is most likely that silicon carbide at the surface was removed by sublimation prior to the tungsten powder melt. No diffusion of tungsten into silicon carbide was observed.

In the case of stationary heating (not scanning), all tungsten coated specimens with pre-treatments were stable following IR processing, while cracks were observed to propagate into the substrate and the specimens broke into several pieces for most specimens without the pre-treatments during IR processing. Even in the case of the broken specimens, the coating was not peeled from the silicon carbide substrate, indicating a very adherent layer was formed. In the 'pretreated' cases, the critical ingredient appears to be the vapor deposited tungsten layer. The addition of a very thin titanium layer under the vapor deposited tungsten was used in the hope of aiding the wetting of tungsten to silicon carbide. It has been reported that the reaction between tungsten and silicon carbide occurs above 1200 °C, leading to a bulk diffusion path $W/W_5Si_3/WC/SiC$ [7]. The thickness of those regions depends on temperature and time. In this work it was assumed that a reaction layer several hundred nm thick was formed at the interface. However, given the apparent removal of surface silicon carbide through sublimation and the absence of titanium (using EDS), it is felt that the use of titanium and the annealing was unnecessary.

The IR processing conditions were optimized using a series of specimens without pre-treatments (tungsten vapor deposition). The maximum power needed to melt the powder was fixed to 23.5 MW/m^2 for 3 s, which is the minimum time to melt and

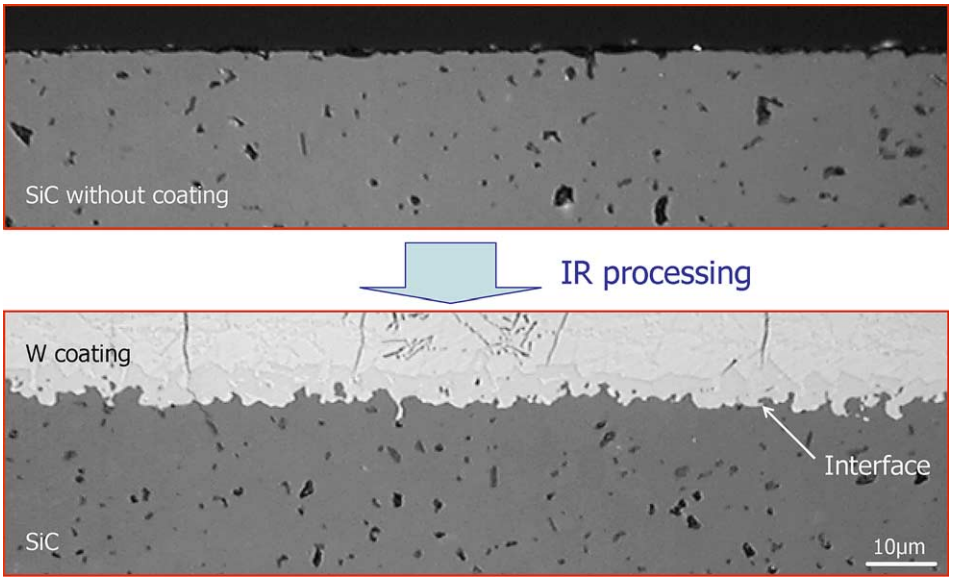

Fig. 1. Effect of IR processing on SiC surface roughness (OM images).

form a continuous tungsten coating for the power. Pre-heating and post-heating at reduced power was used to decrease thermal shock, since the specimen without tungsten vapor deposition was broken into several pieces during IR processing, as mentioned above, in the case of heating at 23.5 MW/m^2 for 3 s. Post-heating in all conditions did not improve the stability of specimens during IR processing, with all samples fracturing into several pieces similar to specimens without post-heating. In contrast, pre-heating at 5.2 MW/m^2 for 20 s improved the stability of specimens, and the specimens with the pre-heating was stable following IR processing, while the specimen with pre-heating at 5.2 MW/m^2 for 10 s did not work well and the substrate broke during IR processing. Fig. 2 is an OM (Nomarski) image showing the effect of tungsten vapor deposition and pre-heating on crack propagation into silicon carbide. In the specimen without tungsten deposition and pre-heating, large cracks induced from the tungsten surface propagated into the silicon carbide substrate (a), while cracks induced from the tungsten surface did not reach the W/SiC interface in the specimens with tungsten vapor deposition (b) and pre-heating (c). Even in the case of specimens without tungsten deposition and pre-heating, cracks did not propagate into the W/SiC interface, while the crack in the substrate propagated parallel to the interface as shown in (a). This was due to the expansion of silicon carbide near the interface, keeping the rest of silicon carbide substrate cool. It is assumed that the tungsten powder was porous prior to the IR processing, allowing part of the energy to be absorbed by the silicon carbide substrate and causing expansion of the silicon carbide near the interface, with crack propagation at cooling. Slowing down the cooling by reducing the lamp power did not prevent the armor and substrate cracking. As a result, pre-heating reduced the propagation of cracks into the silicon carbide. By adding a thin tungsten layer by vapor deposition, it is thought that the IR power is not effectively coupled to the silicon carbide substrate, reducing expansion of the silicon carbide near the surface. This means that part of the silicon carbide substrate surface is more rapidly heated without tungsten vapor deposition.

Fig. 3 shows a back scattering (composition) electron image of a specimen with pre-heating (5.2 $MW/m^2 + 23.5\ MW/m^2$) and without tungsten vapor deposition formed by still heating. The SEM observation reveals a complicated microstructure within the tungsten coating. Through EDS analysis, it was found that grains adjacent to the

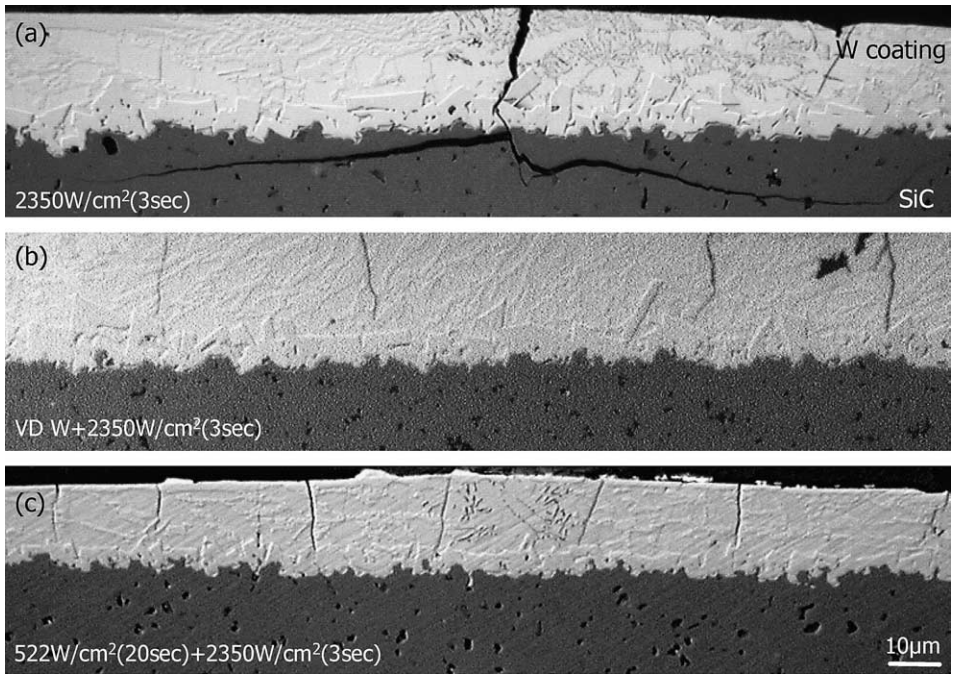

Fig. 2. Effect of vapor deposited W and pre-heating on crack propagation into SiC (a) without pre-treatment, (b) with W vapor deposition, (c) with pre-heating.

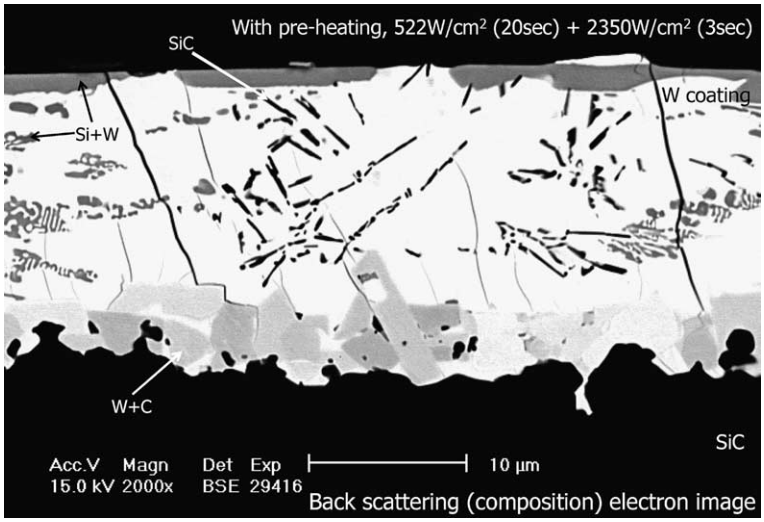

Fig. 3. Typical SEM image (back scattering electron image) of W coating on SiC with pre-heating (5.2 MW/m^2 + 23.5 MW/m^2) and without W vapor deposition formed by still heating.

W/SiC interface within the tungsten coating were tungsten carbide. The W_5Si_3 grains were found near the surface. Silicon carbide grains were also found within the tungsten coating. It is assumed that the sublimated silicon carbide at the interface decomposed and reacted within the melted tungsten. It has been reported that tungsten was coated on silicon carbide successfully by other methods. However those tungsten coatings included relatively thick reaction layers of tungsten and C and tungsten and silicon [7–9]. Those reaction layers cause fracture at the interface by residual thermal stress, attributed to mismatch of the CTE. For this reason, tungsten coating with thin reaction layers is preferred. Through IR processing, the reaction layer was not formed at W/SiC interface, although relatively small reacted grains less than 10 μm were observed. This grain structure can reduce the crack initiation by CTE mismatch compared with the reaction layers, since the stress caused by CTE mismatch distributes to each grain boundary.

Tungsten powder on a silicon carbide substrate was also heated by scanning of the IR lamp forming tungsten coatings of 50–100 μm in thickness. By increasing the scanning speed, the power imparted to the sample is reduced. The scanned heating is

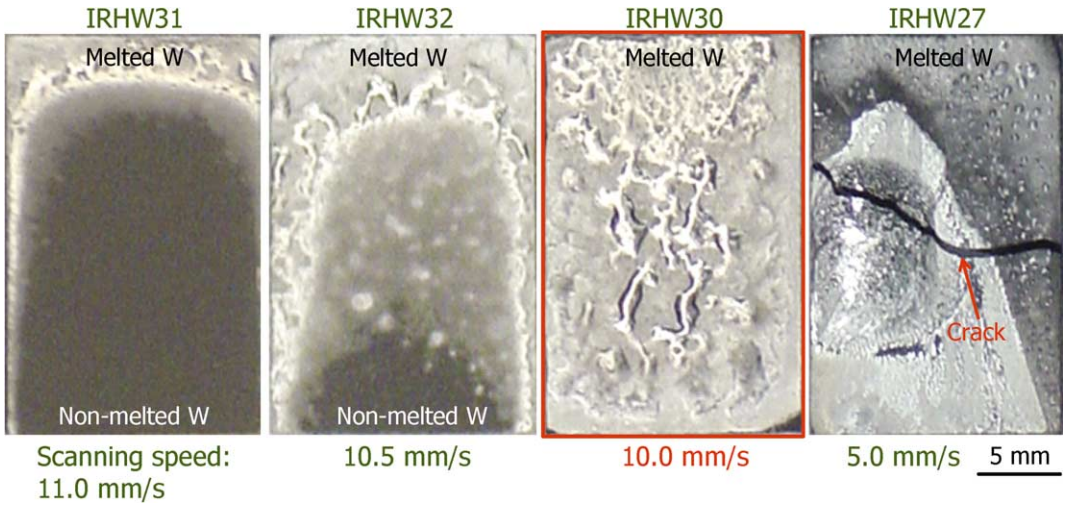

Fig. 4. Effect of scanning speed on coating surface.

more attractive compared to static heating, since it can cover a much larger area. The tungsten vapor depositions specimens without any pre-treatment were used for optimization of the lamp power and scanning speed. Fig. 4 shows tungsten coating surfaces of specimens without any pre-treatment heated by various scanning speeds with a lamp power of 23.5 MW/m^2. Slower scanning speed enhanced tungsten melting, however cracks were induced and the specimen was broken as shown in the IRHW27 specimen. The cross sections of the other specimens, IRHW 31, 32 and 30 scanned at 11.0, 10.5 and 10.0 mm/s, respectively, were observed by FE-SEM as shown in Fig. 5. The cross

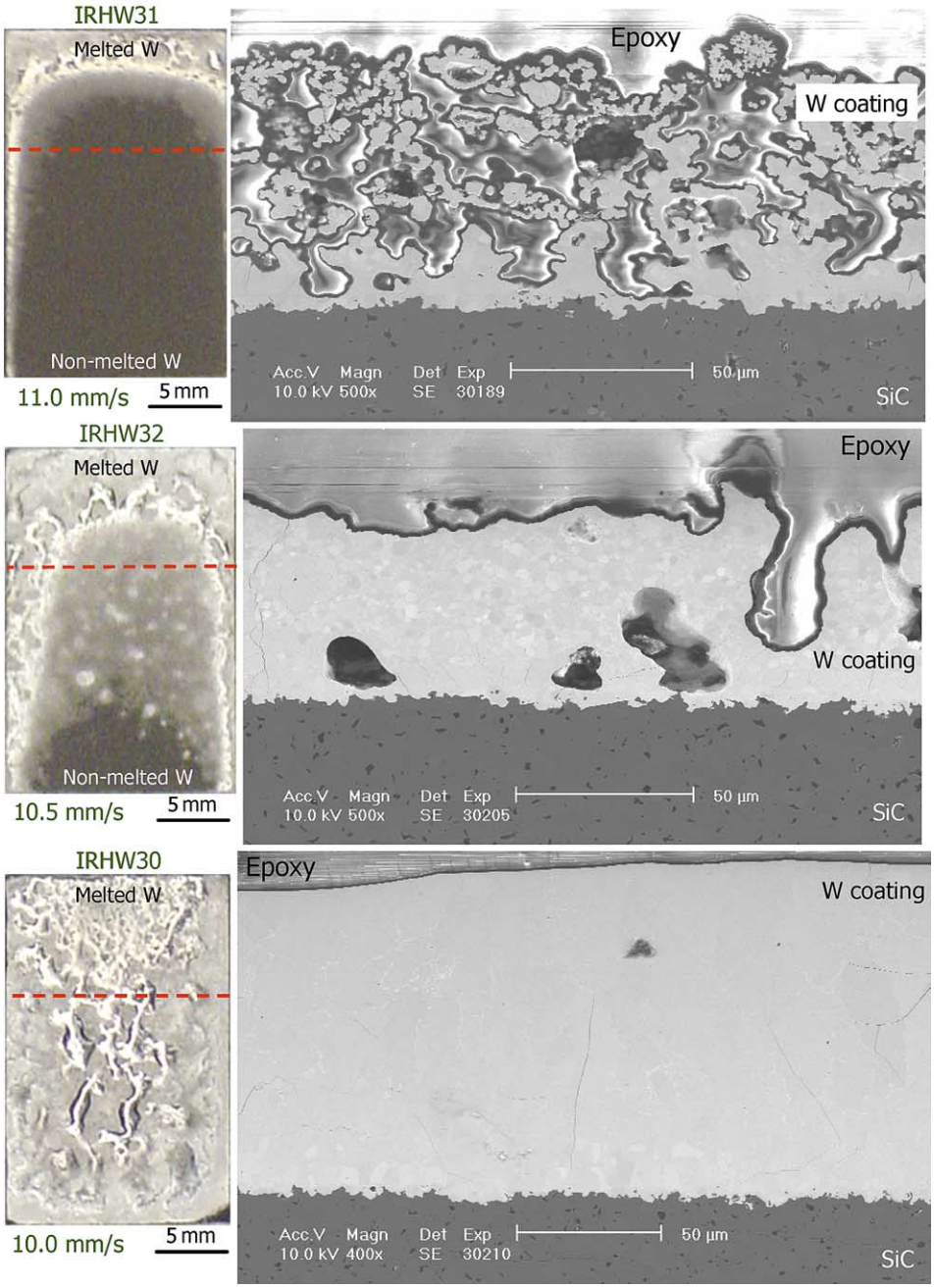

Fig. 5. Cross sectional SEM images of W coatings formed at 23.5 MW/m^2 of lamp power and 11.0 (IRHW31), 10.5 (IRHW32) and 10.0 (IRHW30) mm/s of scanning speed.

sections near the center of the dashed lines were observed. In IRHW31, tungsten was partly melted and a coating was formed near the interface, while the other regions are quite porous with non-reacted tungsten powder. In the melted region adjacent to the interface, tungsten carbide grains, as shown in Fig. 3, were observed, while the other reaction grains and silicon carbide were not observed in the tungsten coating region. There was complete tungsten powder melting with large pores for the conditions in sample IRHW32. In the melted region adjacent to the interface, tungsten carbide grains were observed, while the other reaction grains and silicon carbide were not observed in the tungsten coating region. In IRHW30, complete tungsten melting was observed and a dense coating was formed. In the melted region adjacent to the interface, tungsten carbide grains were observed, while the other reaction grains and silicon carbide were not observed in the tungsten coating region. For the conditions shown in IRHW30, it was determined that the optimum lamp power was 23.5 MW/m^2. A dense tungsten coating was formed at the fastest scanning speed (i.e. the shortest reaction time). Faster scanning speeds than the optimum induces large pores in the tungsten coating as shown in sample IRHW32 in Fig. 5. Slower scanning speed induces extra cracks, as shown in sample IRHW27 in Fig. 4. The optimum scanning speed was obtained for the lamp power ranging from 17.0 to 23.5 MW/m^2, as shown in Fig. 6. Lower power required slower scanning speed, which means longer heating time. Tungsten required more power to melt than molybdenum due to the higher melting point.

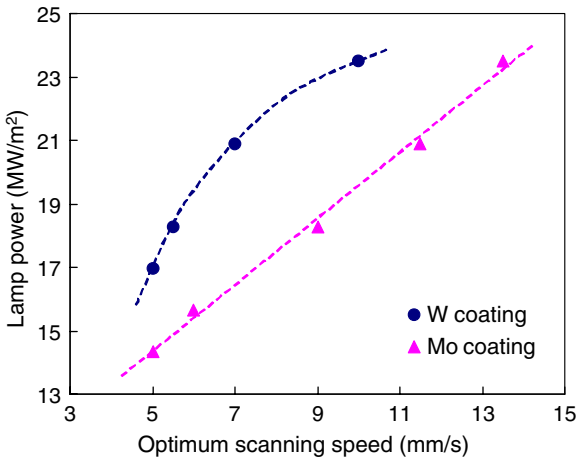

Fig. 6. Relationship between lamp power and optimum scanning speed for W coating and Mo coating.

Microstructures of the tungsten coating without tungsten vapor deposition formed at higher power and shorter heating time (faster scanning speed) and that formed at lower power and longer heating time (slower scanning speed) were examined. Fig. 7 shows back scattering SEM images of the tungsten coating formed at 23.5 MW/m^2 of lamp power and at 10 mm/s of scanning speed. The silicon carbide region is shown as black contrast. Although micron size tungsten carbide particles were observed along the interface within the tungsten coating, a thick tungsten and C reaction layer and a thick tungsten and silicon reaction layer, normally formed by the other coating methods, were not formed. The silicon carbide grains and W_5Si_3 grains observed within the tungsten coating, which were formed at 23.5 MW/m^2 by static heating as shown in Fig. 3, were not observed. Fig. 8 shows back scattering SEM images of the tungsten coating formed at 18.3 MW/m^2 of lamp power and at 5.5 mm/s of scanning speed. The grains of tungsten carbide were observed adjacent to the interface without thick layers of tungsten carbide and W_5Si_3. In addition, relatively large scattered tungsten carbide grains were observed in the coating through the thickness. A eutectic structure of tungsten and silicon was also observed. This implies that the temperature decreased relatively slowly, inducing solidification at different temperature. As shown in the specimens formed by static heating, pre-heating was required to reduce the cracking within the coating and substrate. The scanned heating includes pre-heating and post-heating by conduction from the heated region. As a result, the crack was reduced by scanned heating.

Fig. 9 shows the flexural strength of the tungsten coated specimens formed by scanned heating using the optimized condition for lamp power. The strength of the specimens without tungsten vapor deposition is compared with that of the specimens with tungsten vapor deposition. Error bars show one standard deviation. Scanning speed is in inverse proportion to heating time. Tungsten coating was not peeled off during the flexural test, showing strong interfacial bond. Strength of the silicon carbide substrate decreased during the processing. Dependence of heating time (scanning speed) on strength was not clear, although the strength seems to increase slightly with increase of the scanning speed. As discussed above, tungsten vapor

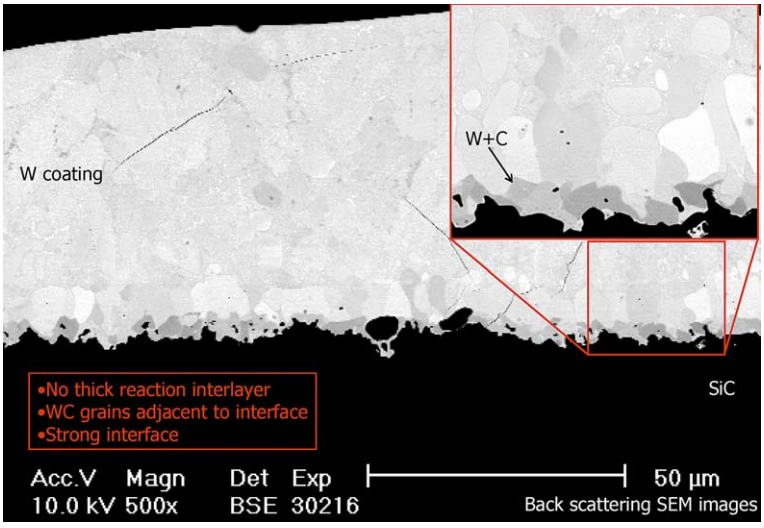

Fig. 7. SEM images of W coating processed at 23.5 MW/m^2 of lamp power and 10 mm/s of scanning speed.

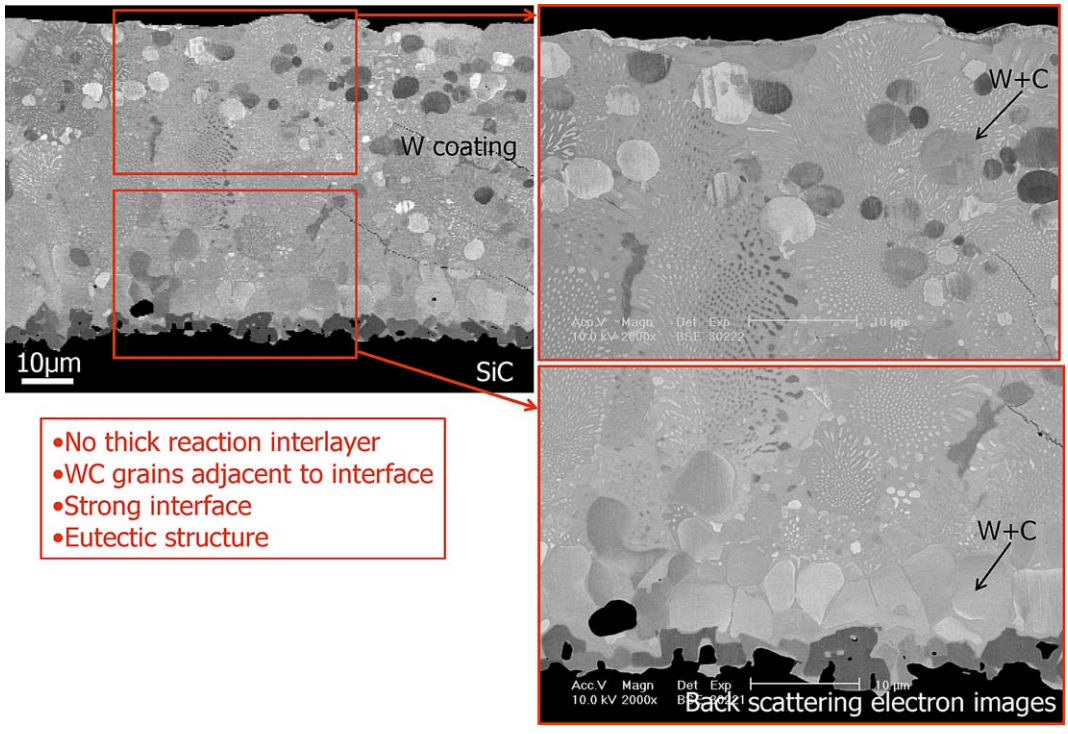

Fig. 8. SEM images of W coating processed at 18.3 MW/m^2 of lamp power and 5.5 mm/s of scanning speed.

deposition was effective in preventing cracks into the silicon carbide substrate. The scanned heating was also applied to the specimens with tungsten vapor deposition. Vapor deposition of tungsten prior to powder coating prevented degradation of the strength slightly. One of the reasons for degradation of the strength by the heating is crack propagation into the silicon carbide substrate, attributed to direct heating of the silicon carbide substrate without tungsten vapor deposition. It was a consistent result that the strength of the tungsten coated specimen with vapor deposition was larger than that

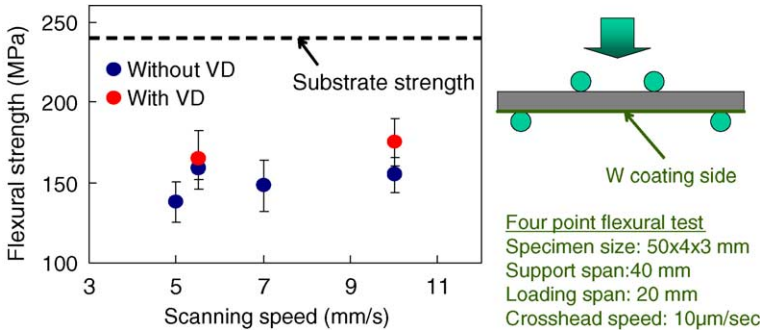

Fig. 9. Effect of processing condition on flexural strength of W coated SiC and the schematic of the four-point flexural test.

without vapor deposition. From the view point of mechanical strength, the specimens formed by faster scanning speeds (shorter reaction time) and with vapor tungsten deposition were superior, although the effect of scanning speed and tungsten vapor deposition on strength was limited.

3.2. Molybdenum coating

Most of the molybdenum coatings applied by IR processing at the same condition used for tungsten coating sublimated due to excessive heating. These included specimens with molybdenum vapor deposition prior to powder coating. Fig. 10 shows OM images of the remaining molybdenum coating (a, b) and the debonded interface (c) of the specimen with molybdenum vapor deposition, heated again at 23.5 MW/m^2 for 3 s. The reaction layer of MoSi determined by EDS analysis was formed at the Mo/SiC interface. The difference in the CTEs of molybdenum and silicon carbide is larger than that of tungsten and silicon carbide. The reaction layer

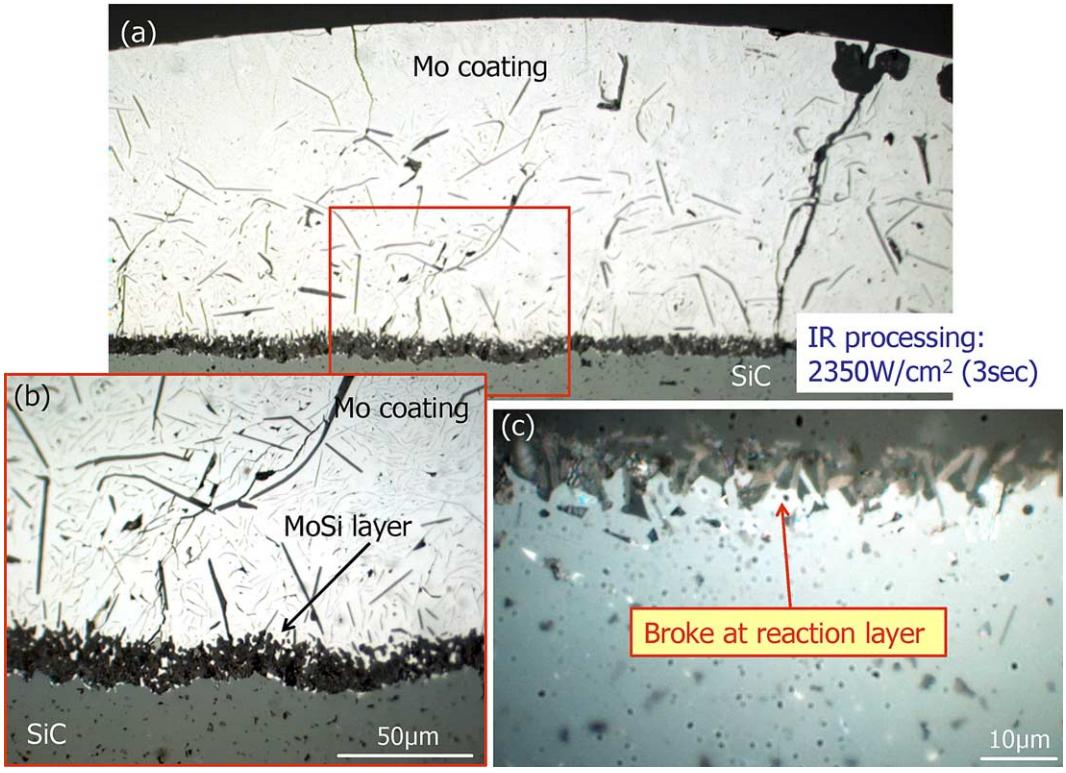

Fig. 10. Mo coating on SiC (a,b) and debonded surface of SiC (c). The specimen was coated by Mo vapor deposition prior to powder coating and heated still at 23.5 MW/m^2 for 3 s.

could not withstand the stress attributed to the CTE mismatch during cooling. The heating condition by IR processing was optimized in the scanning mode. The optimum scanning speed (i.e. the fastest scanning speed to form the coating) was determined in the same way as for the tungsten coating and results are shown in Fig. 6. Most of the molybdenum coating remained following the processing by the optimization. However even with optimization, a reaction layer of MoSi formed and the molybdenum coating was partly peeled off. Coating of silicon carbide with molybdenum proved to be more difficult than with tungsten.

4. Conclusions

A tungsten coating was formed successfully on a silicon carbide substrate. The silicon carbide substrates without pre-treatment or pre-heating were broken during IR processing in the case of static heating. It was found that vapor deposition of the tungsten prior to powder coating and pre-heating at lower power mitigated crack propagation into the silicon carbide substrate. Scanned heating also prevented cracking of the tungsten coating and silicon carbide substrate as shown in the pre-heating sample heated statically. It was found that a porous tungsten coating is formed by insufficient reaction time and that the silicon carbide substrate tends to break if the reaction time is too long (for constant heat flux). The scanning speed and processing time were optimized for lamp powers with 17.0–23.5 MW/m^2.

Tungsten carbide grains were formed near the interface within the tungsten coating in all specimens, while silicon carbide grains and the W_5Si_3 grains were observed in the middle and surface of the tungsten coating in the case of static heating. While tungsten carbide grains were observed along the interface within the tungsten coating in all samples, relatively large scattered tungsten carbide grains and eutectic structure of tungsten and silicon were observed only in the coating formed by lower lamp power and longer heating time in the scanning mode. It was found that a thick reaction layer, which causes thermal residual stress due to CTE mismatch, was not formed.

Tungsten coatings were not peeled off during flexural tests, indicating a strong interfacial bond. Strength of the silicon carbide substrate decreased during the processing. The strength seems to increase slightly with increase in the scanning speed. Vapor deposition of tungsten prior to powder coating prevented degradation of the strength slightly.

Most of the molybdenum coatings sublimated due to excessive heating. Furthermore, a reaction layer of MoSi, which may have enhanced crack propagation, was observed. The formation of a molybdenum coating proved much more challenging than tungsten coatings on silicon carbide using the Infrared Transient Liquid Phase Processing.

Acknowledgement

This work was sponsored by the Department of Energy's High Average Power Laser Program.

References

[1] T. Noda, J. Nucl. Mater. 233–237 (1996) 1475.
[2] L.L. Snead, R.H. Jones, A. Kohyama, P. Fenici, J. Nucl. Mater. 233–237 (1996) 26.
[3] A.R. Raffray, D. Haynes, F. Najmabadi, J. Nucl. Mater. 313–316 (2003) 23.
[4] Y. Ueda, K. Tobita, Y. Katoh, J. Nucl. Mater. 313–316 (2003) 32.
[5] <http://www.hexoloy.com/>.
[6] <http://www.matweb.com/>.
[7] F. Goesmann, R. Schmid-Fetzer, Mater. Sci. Eng. B 34 (1995) 224.
[8] K.M. Geib, C. Wilson, R.G. Long, C.W. Wilmsen, J. Appl. Phys. 68 (6) (1990) 2796.
[9] S.J. Son, K.H. Park, Y. Katoh, A. Kohyama, J. Nucl. Mater. 329–333 (2004) 1549.
[10] C.A. Blue, V.K. Sikka, E.K. Ohriner, P.G. Engleman, D.C. Harper, JOM-e 52 (1) (2000).